Fabrication of 3D nanoimprint stamps with continuous reliefs using dose-modulated electron beam lithography and thermal reflow

2010 J. Micromech. Microeng. 20 095002

(http://iopscience.iop.org/0960-1317/20/9/095002)

J. Micromech. Microeng. **20** (2010) 095002 (6pp) doi:10.1088/0960-1317/20/9/095002

Fabrication of 3D nanoimprint stamps with continuous reliefs using dose-modulated electron beam lithography and thermal reflow

Arne Schleunitz and Helmut Schift

Paul Scherrer Institut, Laboratory for Micro- and Nanotechnology, 5232 Villigen PSI, Switzerland

E-mail: arne.schleunitz@psi.ch and helmut.schift@psi.ch

Received 4 June 2010, in final form 30 June 2010
Published 5 August 2010
Online at stacks.iop.org/JMM/20/095002

Abstract
3D electron beam lithography and thermal reflow were combined to fabricate structures with multilevel and continuous profiles. New shapes, smooth surfaces and sharp corners were achieved. By using exposure with variable doses, up to 20 steps were fabricated in a 500 nm thick resist with a lateral resolution of 200 nm. Steps were reflowed into continuous slopes by thermal post-processing, and were transferred into silicon substrates by proportional plasma etching. The method can be used for the fabrication of 3D nanoimprint stamps with both sharp features and continuous profiles.

1. Introduction

Electron beam lithography (EBL) allows three-dimensional (3D) patterning by using dose-modulated exposure and adapted wet development [1]. Depending on the dose D deposited in the depth of the resist, the molecular weight M_w of the polymer is reduced in the exposed areas of a thin layer of a positive resist such as poly(methyl methacrylate) (PMMA) [2]. During development, this allows the removal of parts of the exposed resist with a high M_w selectivity due to their varied ability to dissolve in the developer, while the non-exposed resist remains unaltered. The depth of the development is determined by using a specific development time t_{dev} in a low contrast developer, which exhibits M_w dependent etch rate. Thus, multilevel staircase structures can be generated if the dose variation in adjacent exposure fields results in a sufficiently distinct M_w variation. Low depth will be achieved in locations with high M_w and high depth in locations with low M_w. Due to narrow beam and low scattering they will be laterally and vertically separated with sharp corners [3–5].

In addition to lithography, thermal reflow techniques can be used as a simple and well-established post-processing method for modifying the shape of a binary (i.e. one-level) resist structure fabricated by photolithography (PL) or EBL into a 3D shape. Resist melting and mass transport of thermoplastic photoresists are already used widely for the fabrication of spherical or cylindrical lenses in the micrometer range with very smooth surfaces in wafer scale [6]. When heated over its glass transition temperature T_g, the resist changes into a viscous state and surface tension leads to the formation of a surface of the least energy (surface of minimum area). In [5–8] reflow was also used for surface smoothening and roughness reduction.

In [9, 10] mass transport was done with micrometer-sized multilevel structures. Prismatic gallium phosphide optics with smooth sidewalls and 8.2 μm high, 100 μm long slopes (with 4.7° angle) were created from five 1.6 μm high, 20 μm wide steps. Here, instead of heating the entire structure, local heating by laser exposure was used. This had the advantages that only the surface part of the structure deforms while the bulk part remains unaltered.

In the research described in this paper, we present a new process route for the fabrication of 3D structures which exhibit both sharp and continuous profiles. This was previously not feasible by standard grayscale EBL which is restricted to manufacture only (quasi-) multistep patterns. The new method is based on the combination of grayscale EBL with a moderate thermal reflow process. In contrast to [4], the 3D originals were fabricated by dose-modulated EBL in a polymeric resist with lateral resolutions below 200 nm, and thermal reflow was

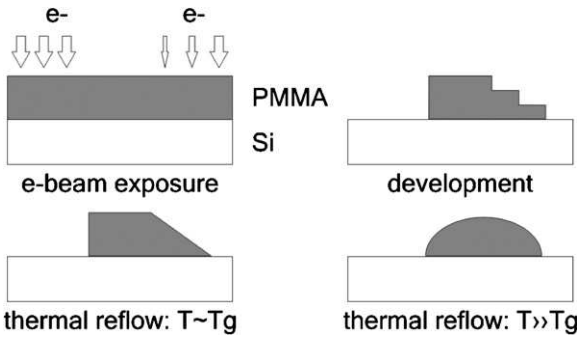

Figure 1. Process chain or schematic: different 3D shapes with sharp and continuous profiles can be achieved from an e-beam exposed resist structure by choosing the appropriate reflow temperature.

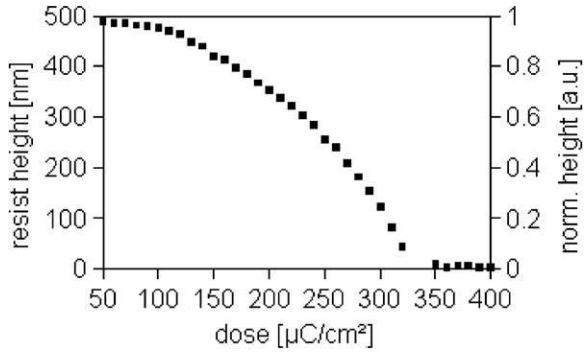

Figure 2. Contrast curve in 500 nm thick PMMA 950 k (the development time of 60 s with developer IPA:MIBK 1:1).

effectuated by global heating at moderate temperatures. The process scheme is depicted in figure 1.

2. Experimental details

All structures presented here have been fabricated in a classical PMMA EBL resist (Allresist AR-P 679.04) with M_w of 950 k (k means kg mol^{-1}), and a thickness of 500 nm. After the exposure (Vistec EPBG 5000+ HR at 100 keV), samples were developed for 60 s in methyl–isobutyl ketone (MIBK) mixed with isopropyl alcohol (IPA) at a ratio of 1:1 to obtain a low contrast in a Hamatech spray developer at room temperature, and rinsed in IPA for 30 s. A dose variation from 0 to 400 μC cm^{-2} was performed in order to determine the dose-depth correlation and plotted according to [5]. Figure 2 shows that for the specific development procedure (developer mixture and duration) the dose for which complete development was achieved (so-called dose-to-clear) was 325 μC cm^{-2}. Here, no PMMA residues remain at the silicon substrate after development. Using this, in a 500 nm thick resist, up to 20 levels with equal depth increments could be fabricated using doses from 50 to 350 μC cm^{-2} (in the following, we will denominate this 'attenuated' case). The smallest depth increment was measured to be 25 nm, and a minimum lateral step size of 200 nm was achieved. While the precision of these steps could be controlled within a few percent, a rough pattern was observed which corresponds partially to the exposure fields defined by the EBL exposure software. Using scanning force microscopy, the depth of this roughness was determined to be around 10 nm. For the following experiments, we did not optimize the exposure setup to remove this roughness, but kept it as a means for improving the effectiveness of the post-processing.

For reflow the resist structures were put on a hot plate and left heated under ambient conditions at a constant temperature. The resist was hardened by instant cooling when the desired shape was achieved. For a better examination the reflow has to be controlled over time. We therefore started with reduced reflow temperature T_{reflow} below the known original T_g, hereof 118 °C, to avoid rapid collapsing of structures, and observed structure evolution over time [11]. Higher temperatures lead to more rapid reflow, but also to a more pronounced deformation of the entire structures. A process window was defined to be between 100 and 140 °C (here at 15 min process time). Resulting process steps are shown in figure 3, for a pyramid with four steps in a 585 nm high resist with lateral step sizes of 1 μm.

(a, b) For temperatures below and up to 100 °C, no shape deformation due to the thermal treatment is observed.

(c) At 110 °C, the onset of smoothening of surface roughness can be seen; surface roughness due to EBL exposure and development is smoothened out.

(d) At 115 °C, smoothening is complete and onset of structural deformation can be seen (particularly at the corners). Non-exposed areas can still be clearly distinguished from exposed areas (sharp edges).

(e) At 120 °C, steps of a few 10 up to 100 nm are deformed and smooth continuous surfaces appear. Non-exposed areas can still be distinguished from exposed areas, suggesting that there is still no flow within non-exposed areas at this temperature, but corners are slightly smoothened out.

(f) At 140 °C, entire structures are deformed with smooth continuous surfaces. Non-exposed areas are also beginning to be deformed.

3. Reflow of structures with molecular weight modulation

In the following, before we come to the discussion of the different cases, we will deduce some further parameters from different sources, which serve as guidelines for process evaluation and interpretation, and enable to judge the orders of magnitudes of effects. We do not claim to give a conclusive picture about all effects, or to provide exact quantitative data on M_w, T_g or viscosity $\eta_0(T)$ for the PMMA resist used here.

In the case described in [12], thermal reflow was applied in microstructures with local M_w modulation. This allows reflowing of areas with low M_w, while others remain insensitive to reflow due to their high M_w. For high cylindrical resist pillars in PMMA by deep x-ray lithography, x-ray flood exposure was used as post-processing to reduce the molecular weight at the top of the structure while the bottom remained

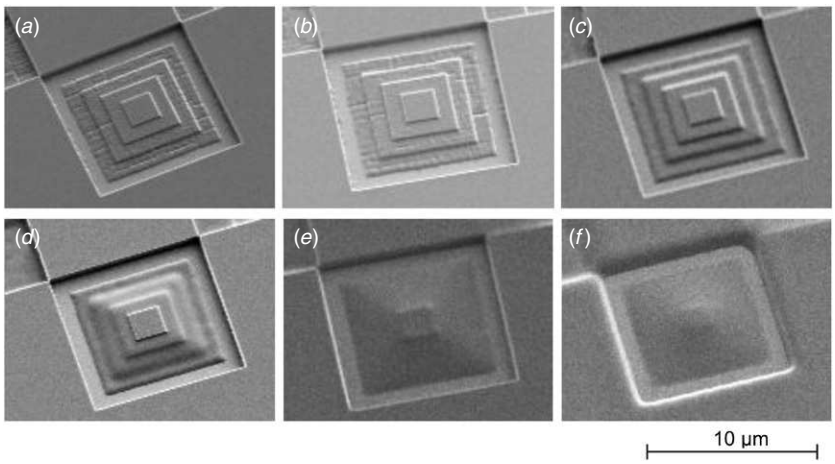

Figure 3. Reflow temperature study with a stepped pyramid with four exposure dose levels at (*a*) 25, (*b*) 100, (*c*) 110, (*d*) 115, (*e*) 120 and (*f*) 140 °C.

almost unexposed. The local absorption in the pillars was chosen in a way that the threshold for M_w and consequently a low enough viscosity $\eta_0(T)$ needed for reflow was reached in the upper part of the pillar. During reflow, only the top of a pillar was melted and resulted in a high base cylinder with a spherical top.

In x-ray exposure, photons are absorbed following an exponential absorption law, thus resulting in a continuous decrease of dose down to the bottom of the resist [13]. In contrast to this, for high-energy electron beams and thin films, as were used in the investigations described here, the absorbed energy density is approximately uniform in the full depth of the resist. This is particularly valid for the thin (below 1 μm) resist structures and the 100 keV electrons used here, with low forward scattering into adjacent areas. As in XRL, in EBL linear polymers with high M_w of 50 k and higher are exposed. In both cases, after exposure, M_w below 10 k is needed to enable the attack of the appropriate developer [2].

It is known that T_g of PMMA can vary significantly between 85 and 165 °C due to the vast number of commercial compositions [14]. For example for molding processes such as nanoimprint lithography (NIL), PMMA of M_w 25 k or 75 k with a typical T_g of 105 °C is used [15]. In [16] we can find for isotactic PMMA that T_g for low M_w is much lower than for higher M_w, i.e. for 1.45 k, 4.9 k, 11 k, 21 k and 55.9 k, T_gs of 42, 93, 118, 119 and 121 °C were measured, respectively. Note that while for lower M_w lower than 10 k a drop in T_g is observed, above 10 k no significant dependence of T_g on M_w can be found. The same behavior was also found for the 950 k PMMA used here with T_g of 118 °C [11]. M_w lower than 10 k, needed for development after EBL exposure [2], is exactly in the range where large differences in T_g can be found. This is in accordance with the minimum M_e, above which entanglement of PMMA chains becomes significant, and thus an increase of chain interaction, since below M_e the chains are composed by only 100 monomer entities [17]. This is particularly important if PMMA has to be molded in its viscous state, i.e. above T_g, where chain mobility is increasing due to a loss of entanglement. Therefore, we anticipate here that a similar behavior is found for all kinds of PMMA.

For NIL as well as for standard reflow, another property becomes important. Here, process temperatures are chosen in the purely viscous flow regime above a flow temperature T_f, which is 30–60 °C above T_g, at which the viscosity is low enough to ensure flow. For entangled polymers (T_g above 10 k), it is known that this T_f is dependent on M_w, while T_g is considered as almost independent of M_w. This means that for standard reflow processes, M_w modulations will result in differences in flow [11]. In [17] we can also find that the viscosity for lower M_w is much lower than for higher M_w, e.g. for 7 k, 26 k, 71 k, 151 k and 396 k viscosities of 2100, 66 810, 101 000, 167 400 and 421 000 Pa·s were measured at 200 °C and at a shear rate $\dot{\gamma}$ of 10 s^{-1}. The values for 26 k to 71 k are 10 to 20 times higher than those measured in [18], which shows that the dependence on polydispersity M_w/M_n, tacticity or experimental tolerances have to be taken into account.

According to [2, 19], the fragmented polymer chains with sufficiently low M_w after e-beam exposure are almost independent of the initial M_w if the initial M_w is higher than 50 k. M_w of PMMA resists used in EBL is usually larger than 50 k; therefore, this rule applies for almost all practical cases, and particularly for the EBL resist used here. Then, for the threshold dose for the development $D_{\min}$ of PMMA used in EBL, the high initial M_w needs to be reduced to below 10 k. It was also found that then $(M_w)^{-1}$ is linear with dose, meaning that if 10% is the minimum dose needed for the development for the smallest step, for 100% M_w will be even ten times smaller, i.e. 1 k for 100% dose, if the threshold for development is 10 k. Because of the fact that M_w is equal to or below 10 k for both cases, the full dose and the attenuated case, we therefore anticipate here that both T_g and T_f will be dependent on M_w; furthermore, the visco-elastic flow regime (between T_g and T_f) will be rather limited, and significant flow can be achieved already at relatively low temperatures above T_g, or more precisely, $T_g(M_w)$. Since in this publication we are interested in modifying EBL exposed, multilevel structures within a 'global' process, i.e. a full wafer non-localized heating process, we need to take these assumptions into account. Note that for the parameters chosen for the current research, as will be described in the following, the etching speed during

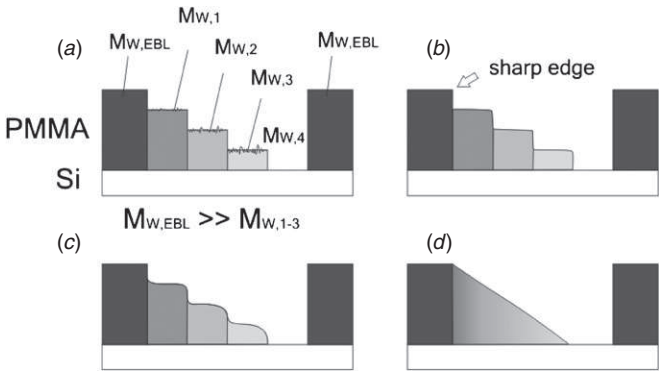

Figure 4. Schematic of the M_w distribution after EBL and polymer behavior during the reflow process at different temperatures: (*a*) structure after EBL development, (*b*) smoothening, (*c*) beginning of reflow, (*d*) development of continuous slope.

development is not proportional to the dose, and consequently not to $(M_w)^{-1}$.

As a consequence, this means exposure of almost any high M_w resist results in quite low M_w, and therefore it can be anticipated that by exposing a specific pixel area $A(x, y)$, its properties can be defined according to the following chain: higher $D_{\text{exp}}(x, y) \rightarrow$ lower $M_w(x, y) \rightarrow$ lower $T_g(x, y)$ and lower $T_f(x, y) \rightarrow$ lower $\eta_0(x, y, T)$.

4. Discussion

In the following, we apply this knowledge to the pyramidal structures shown in figure 3. At first glance, the process latitude for reflow is large enough to allow the modification of an original multistep structure in different ways. For the relatively shallow microstructures shown here, with step sizes around ten times larger than step depths, the experiments exhibit a quite distinct behavior. There are five areas of interest (see figures 4 and 5):

(a) Figure 4(*a*): a stepped structure is generated after exposure and development with locally different and clearly distinguished M_w. The dose and development time is adjusted such that for highest (100%) dose, the polymer of $M_{w,4}$ is completely removed. In contrast to this, the non-exposed polymer with $M_{w,\text{EBL}}$ is not attacked. In areas with $M_{w,1}$, $M_{w,2}$ and $M_{w,3}$ (the attenuated case), the etch rate is smaller than that in the area of the highest dose, and residual polymer of different heights is covering the substrate. A surface roughness is often generated by machine-induced minimal dose variations during exposure.

(b) Figure 4(*b*): the surface roughness is smoothened out, while the 3D shape is maintained, i.e. the smoothening seem to be self-limited to areas with roughness. This is due to the capillary action which tends to minimize the surface. It is expected that this process is nearly viscous since M_w is very low in the exposed areas. As will be more obvious in figure 4(*c*), the sharp step between exposed and non-exposed structures (indicated by arrow), even for very low (10%) dose ($M_{w,1}$), demonstrates that $\eta_0(T)$ is significantly lowered in the exposed areas. Taking into account measurement published in [2, 17], here M_w is lower than 10 k. T_g and accordingly T_f of exposed and non-exposed structures is different to an extent, that within a temperature difference of a few degrees (i.e. a controlled process regime) a flow regime can be found, where non-exposed areas can still be considered as hard, while exposed areas are already subjected to viscous flow. These sharp edges can be helpful if structures with pronounced and sharp features have to be fabricated, i.e. sawtooth gratings with asymmetric shape and vertical sidewalls. However, the smoothening of these corners should be possible by blurred exposure. Smoothening seems to be complete for roughness and grooves with depth lower than 10 nm. Since this smoothening will also affect sharp corners, it is obvious that structural details below 10 nm will be lost during this process.

(c) Figure 4(*c*): at higher temperatures the smoothening of the steps between the different levels seems to be slightly different, i.e. the steps at the upper levels are sharper than those at the lower levels. This is probably due to the fact that M_w at the lower levels is lower than that

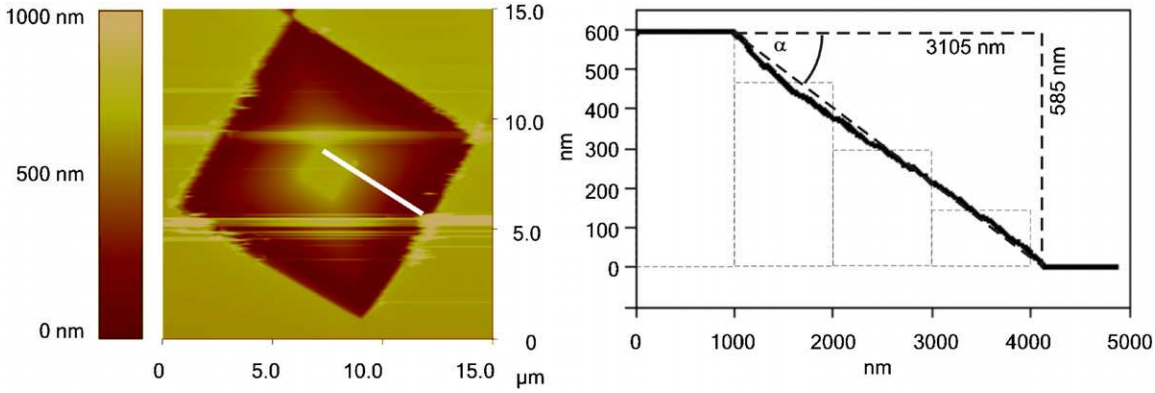

Figure 5. Characterization of the sloped sidewall achieved by the four-level structure (initial steps indicated in profile) and reflow at 120 °C for 15 min, with an angle of $\alpha = 10.7°$.

(This figure is in colour only in the electronic version)

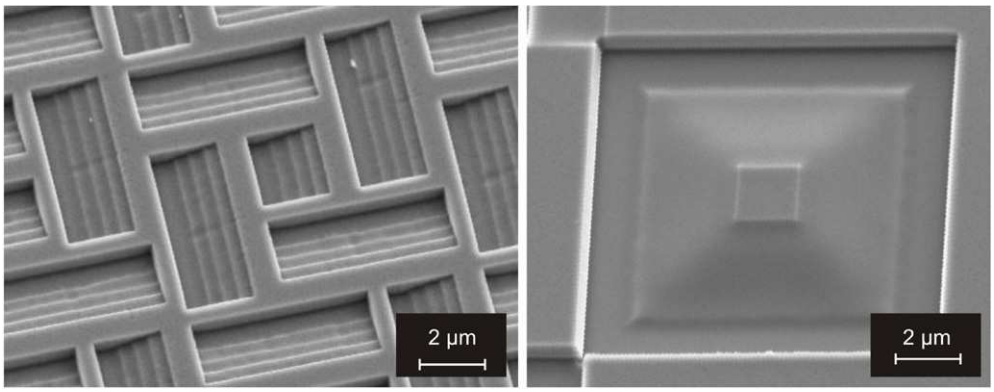

Figure 6. Silicon stamp fabrication by proportional pattern transfer of the resist using RIE. Both staircase profiles (left) and continuous sidewalls (right) are faithfully transferred into the silicon substrate.

in the upper levels, and therefore η_0 is lower at a given temperature. The range of this variation can probably be controlled to some extent during exposure. If only a smoothening of roughness is needed, the aim should be to take the lowest temperature possible for smoothening and to enlarge the time until flow is terminated. Because of the equal tendency that 90° corner grooves will be rounded in the same way as grooves are filled from the side, rounding in the range of the size of grooves is always to be taken into account. However, larger structures will tend to stay as they are. At the bottom of the lowest level, the structure is sharper than between the different levels. This is due to the fact that at the polymer–substrate interface, the difference in the surface energy of polymer toward the substrate (e.g. silicon) determines the contact angle. This can be avoided if the lowest level is not completely removed during development, i.e. slightly below the maximum dose. In contrast to this, the surface energy can be modified by choosing the appropriate substrate or by modifying the surface by plasma treatment or deposition of a hydrophobic coating with molecular vapor deposition before reflow [20].

(d) Figure 4(*d*): currently, with the actual process parameters, a complete smoothening of surface steps, i.e. the formation of a continuous profile, can be achieved from the non-exposed down to the 10% dose level. This is not possible with cross-linked PMMA, which due to its high M_w is not able to flow. As demonstrated in [5] exposure to high temperatures will only lead to rounding of sharp corners. For the four-level structure in figure 4(*a*), the slope linearity seems to be fine (see the measurement in figure 5), and both convex and concave corners are no longer visible (apart from the central non-exposed pillar and at the border to the cleared substrate). The slope is around 10°. Here, the minimum of step (or level) number has to be clarified which ensures the forming of a continuous profile. It can be anticipated that there is an optimum number of steps, increment and step size for which this linearity can be improved. The reason, that rather a linear slope than a meniscus between the steps is formed, lies in the fact that there is volume conservation at very small distances, and there is no significant polymer flow in the bulk. According to [21], it is even possible that smaller features (such as corners) have even lower T_g than the bulk, which would explain this tendency to smoothen out corners. Then we need enough flow so that steps can be smoothened out, but have to restrict flow from one step to the next one.

Without the aim to provide exact quantitative data on local M_w and η_0, we can now sketch the process needed to achieve reflow in EBL exposed multilevel structures: (a) temperatures for reflow should be chosen as low as possible to keep the overall shape of the original and avoid melting of bulky structures. (b) The difference in flow depending on M_w should be low enough to ensure a homogeneous smoothening on each level, but T should be controllable to an extent that different states from smoothening to melting can be achieved in a controlled way. As already shown in [18], the shape should be controllable either by design (e.g. line or dot), flow restrictions (i.e. forming of a defined meniscus, available volume), chemical barriers (high surface energy), temperature (within a range of a few degrees) or careful setting of time (in a continuous evolution within a time window of 1–10 min, a stopping at exact states of reflow should be possible).

5. Stamp fabrication

Figure 6 shows the transfer of the resist structure into silicon using a standard reactive ion etching (RIE) process developed for proportional pattern transfer. The ICP-RIE (Oxford ICP 100) etching process had an etch rate of 50 nm min^{-1}. The M_w variation does not affect the etching rate, which demonstrates that it is determined rather by the density than by the length of the PMMA chains, since their chemical nature is still similar. High (non-exposed) M_w in the center and low (exposed) M_w polymer at the border of the structure is etched with an etch ratio of 1. However, care has to be taken that low M_w is not heated over its T_g during RIE processing and more volatile products are generated with very low M_w.

6. Outlook

The results clearly show the versatility of the process for the generation of various surface profiles which is not possible

with standard lithographies. Its main advantage is that with a global process and volume conservation, structures can be generated which are not easy to fabricate with other methods. The limitations of the process have still to be explored; currently we are obtaining smooth structures with very shallow shapes (10°). Along with the M_w dependence of the flow, both sharp corners (and high resolution) and smooth structures can be fabricated on the same substrate in close vicinity, simply by varying the local exposure dose and leaving others unexposed. Furthermore, slopes with different angles (over steps of a few to 100's of μm) as well as steep (vertical) structures can be fabricated with a single (global) process on full wafer scale. This would be particularly interesting for asymmetric tooth structures, e.g. for blazed gratings with inclined teeth.

The final aim should be to control the complete process chain, i.e. to clarify the dependence of dose to viscosity, but also to simulate the flow during thermal treatment. The latter is particularly difficult for structures with local M_w modulation, because not only lateral etching during development, but also lateral flow between areas of different M_w during reflow has to be taken into account. Tolerances and M_w distribution will also play a role. Whether the minimum resolution can be improved is more a question of optimizing the EBL and development than of the reflow process. However, as is known from other lithographies, there are certainly design restrictions to be considered, e.g. that nanostructures cannot be fabricated in attenuated areas. A trade-off between rounding and resolution is expected. Currently, the possibility of controlling the process within a few degrees of temperature is sufficient to fabricate structures for a range of applications, most prominently optical elements with defined diffractive and refractive properties. These applications range from the improved optical surfaces, where post-processing is used to smoothen out defects and roughness, to holographic structures with continuous profiles and higher diffraction efficiencies.

Acknowledgments

We thank C Spreu, V Guzenko, B Päivänranta and C David (PSI Villigen), for their help and valuable contributions. The research presented here was partially funded by Swiss Federal Office for Science and Education in the framework of the EC-funded project NaPANIL (contract no NMP 214249).

References

[1] Stauffer J M, Oppliger Y, Regnault P, Baraldi L and Gale M T 1992 Electron beam writing of continuous resist profiles for optical applications *J. Vac. Soc. Technol.* B **10** 2526–9

[2] Dobisz E A, Brandow S L, Bass R and Mitterender J 2000 Effects of molecular properties on nanolithography in polymethyl methacrylate *J. Vac. Sci. Technol.* B **18** 107–11

[3] Piaszenski G, Barth U, Rudzinski A, Rampe A, Fuchs A, Bender M and Plachetka U 2007 3D structures for UV-NIL template fabrication with greyscale e-beam lithography *Microelectron. Eng.* **84** 945–8

[4] Kim J, Joy D C and Lee S-Y 2007 Controlling resist thickness and etch depth for fabrication of 3D structures in electron-beam grayscale lithography *Microelectron. Eng.* **84** 2859–64

[5] Teh W H and Smith C G 2003 Fabrication of quasi-three-dimensional micro/nanomechanical components using electron beam cross-linked poly (methyl methacrylate) resist *J. Vac. Sci. Technol.* B **21** 3007–11

[6] Herzig H-P, Kley E-B, Cumme M and Wittig L C 2005 Micro-optics *MOEMS; Micro-Opto-Electro-Mechanical Systems* vol 3 ed M E Motamedi (Bellingham, WA: SPIE) p 614

[7] Lee K K, Lim D R, Kimerling L C, Shin J and Cerrina F 2001 Fabrication of ultralow-loss Si/SiO_2 waveguides by roughness reduction *Opt. Lett.* **26** 1888–90

[8] Mori S, Morisawa T, Matsuzawa N, Kaimoto Y, Endo M, Matsuo T, Kuhara K and Sasago M 1998 Reduction of line edge roughness in the top surface imaging process *J. Vac. Sci. Technol.* B **16** 3739–43

[9] Sinzinger S and Jahns J 2003 Microoptics *Lithographic Fabrication Technology* (New York: Wiley-VCH) p 124 chapter 3

[10] Ballen T A and Leger J R 1999 Mass-transport fabrication of off-axis and prismatic gallium phosphide optics *Appl. Opt.* **38** 2979–85

[11] Keymeulen H R, Diaz A, Solak H H, David C, Pfeiffer F, Patterson B D, van der Veen J F, Stoykovich M P and Nealey P F 2007 Measurement of the x-ray dose-dependent glass transition temperature of structured polymer films by x-ray diffraction *J. Appl. Phys.* **102** 013528 (5 pp)

[12] Ruther P, Gerlach B, Göttert J, Ilie M, Mohr J, Müller A and Oßmann C 1997 Fabrication and characterization of microlenses realized by a modified LIGA process *Pure Appl. Opt.* **6** 643–53

[13] El-Kholi A, Mohr J and Nazmov V 2000 Study of properties of irradiated PMMA by the method of thin sections *Nucl. Instrum. Methods Phys. Res.* A **448** 497–500

[14] Ute K, Miyatake N and Hatada K 1995 Glass transition temperature and melting temperature of uniform isotactic and syndiotactic poly(methyl methacrylate)s from 13 mer to 50 mer *Polymer* **36** 1415–9

[15] Schift H 2008 Nanoimprint lithography: an old story in modern times? A review *J. Vac. Sci. Technol.* B **26** 458–80

[16] Andreozzi L, Faetti M, Giordano M and Zulli F 2005 Molecular-weight dependence of enthalpy relaxation of PMMA *Macromolecules* **38** 6056–67

[17] Petersen K and Johannsmann D 2002 Measurements on the surface glass transition of PMMA from the decay of imprinted surface corrugation gratings: the influence of molecular weight *J. Non-Cryst. Solids* **307–310** 532–7 2002

[18] Madbouly S A, Ougizawa T and Inoue T 1999 Phase behavior under shear flow in PMMA/SAN blends: effects of molecular weight and viscosity *Macromol.* **32** 5631–6

[19] Pratt G J 1975 Glass transition temperature and molecular weight distribution of irradiated polymethymethacrylates *J. Mater. Sci.* **10** 809–13

[20] Schift H, Schleunitz A, Spreu C, Hellbernd K and Lee J-J 2010 Shape control of polymer reflow structures fabricated by nanoimprint lithography *Microelectron. Eng.* submitted

[21] Kahle O, Wielsch U, Metzner H, Bauer J, Uhlig C and Zawatzki C 1998 Glass transition temperature and thermal expansion behaviour of polymer films investigated by variable temperature spectroscopic ellipsometry *Thin Solid Films* **313–4** 803–7